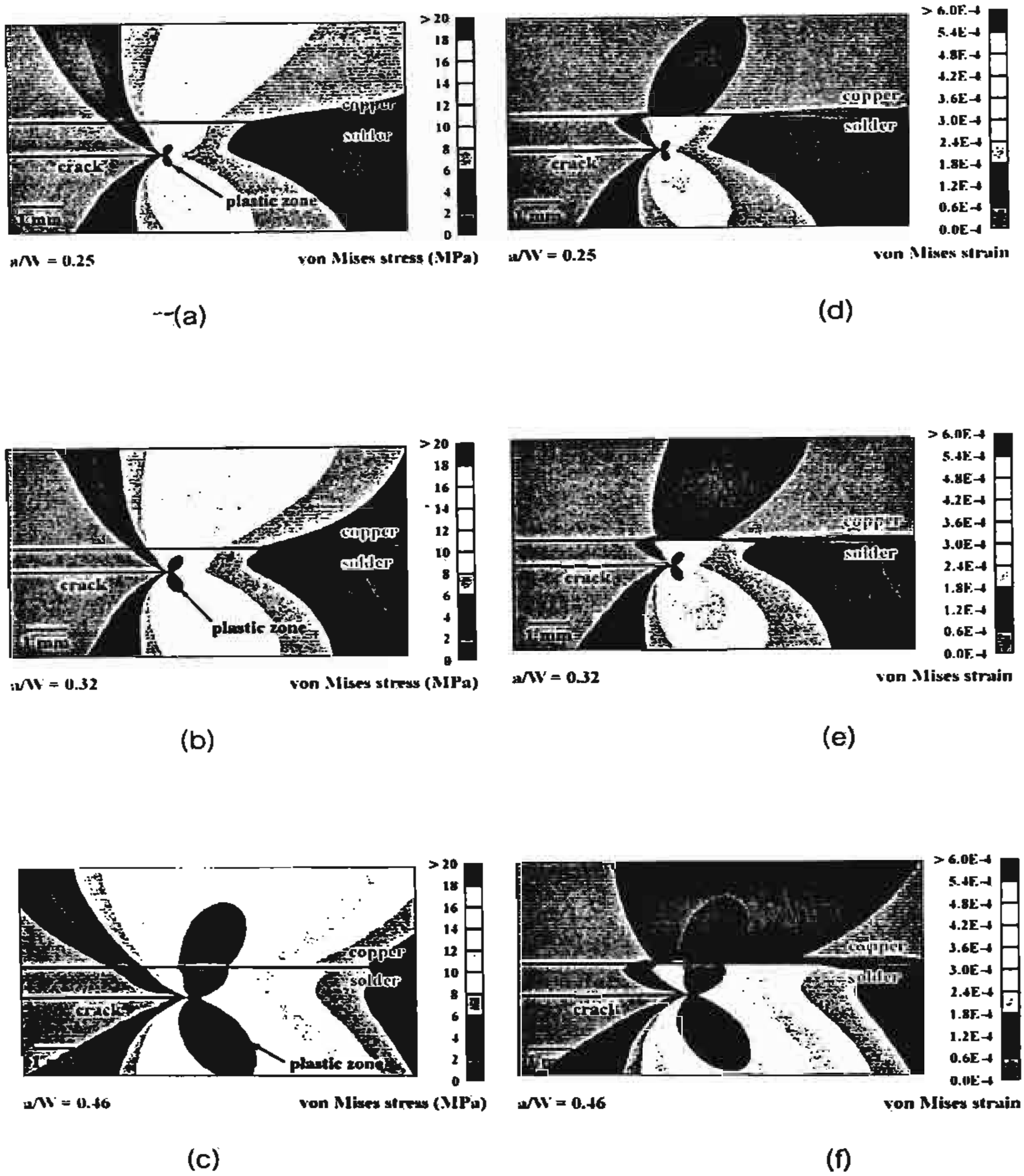

Fig. 10 Von Mises stresses of the specimen for various crack lengths (a) $a/W = 0.25$, (b) $a/W = 0.32$, and (c) $a/W = 0.46$, and Von Mises strains of the specimen for various crack lengths (d) $a/W = 0.25$, (e) $a/W = 0.32$, and (f) $a/W = 0.46$ (loading is in vertical direction).

After some amount of crack propagation in the solder, the crack turned to the interface and propagated along the interface, as shown in Fig. 9. In order to investigate this growth phenomenon, the distribution of von Mises stress and strain near the crack tip at the maximum load for various crack lengths was estimated by using finite element analysis, as shown in Fig. 10. The discontinuity and irregular distribution of the stress and strain are mainly due to the difference of elastic modulus and yield strength between solder and copper. According to von Mises criterion, yielding occurs when von Mises stress reaches the uniaxial yield strength. Since the yield strength of the present solder is 18.1 MPa, the arrows in the solder region of Fig. 10a, 10b, and 10c indicate the plastic zone. The plastic deformation occurs only in the solder side, as can be seen from Fig. 10f. The distributions of von Mises stress and strain along the interface are shown in Fig. 11a and 11b, respectively. It can be estimated from Fig. 11a that the plastic zone ahead of the crack tip reaches the interface when the crack length is longer than *a/W* = 0.42. Based on the experimental result, where the interface debonding occurs at the crack length of *a/W* = 0.46 (critical crack length), the interfacial von Mises stress, i.e. adhesive strength, can be estimated to be 20.2 MPa.

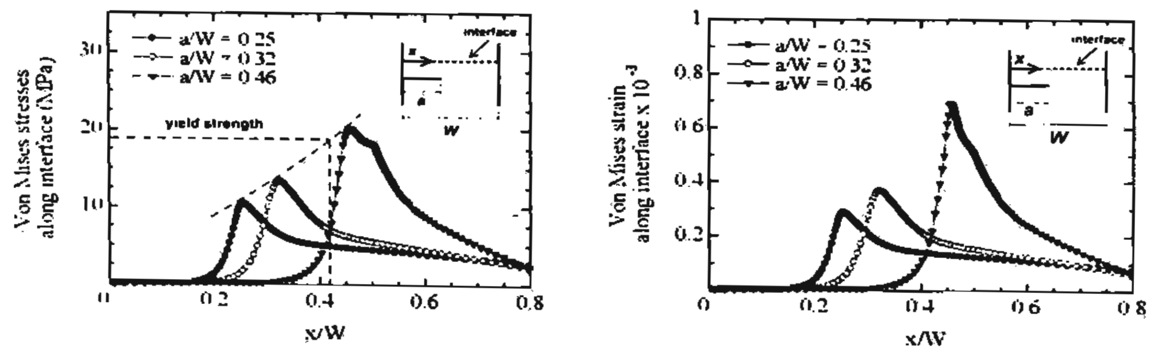

(a) (b)

Fig. 11 (a) Von Mises stresses along interface for various crack lengths, and (b) Von Mises strains along interface for various crack lengths.

Quan et al. (1987) measured the adhesive strength of 60Sn-40Pb with a cross section of 3.18x7.62 mm by tensile test as 82.8 MPa, and became 46.23 MPa after storage at 250 °C for 6 hours. Similar reduction in adhesive strength with increasing storage time was reported by Chiou et al. (1995), and Lee and Chen (2002). Since the size and profile of intermetallic band become thicker and rougher with the increasing storage time, it is likely that the adhesive strength depends on the size and profile of intermetallic band, i.e. become weaker with thicker and rougher intermetallic band, and results in the differences of the adhesive strength among literatures.

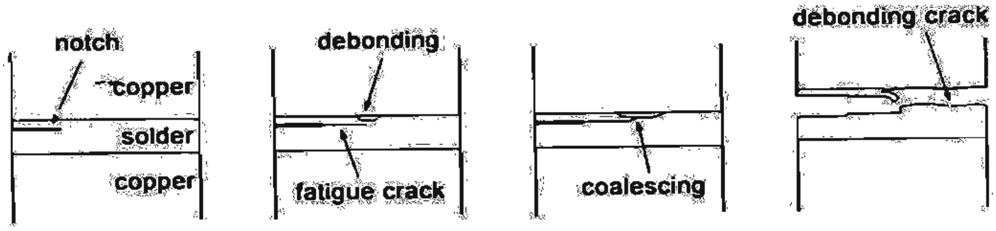

Fig. 12 Schematic of the crack propagation process.

From the foregoing discussion, the crack growth behavior, where the crack turned to the interface and propagated along the interface after some amount of crack propagation in the solder, can be explained as follows. With increasing crack length, the size of plastic zone and the magnitude of stress near the crack tip increase. Consequently, the plastic zone reaches the interface and the stress exceeds the adhesive strength of interface, which results in the interfacial debonding, as schematically shown in Fig. 12. This debonding crack coalesces with the main crack and forms a crack along the interface, which unstably propagates in a brittle manner.

3.5 Conclusions

The behavior and mechanisms of FCG along 63Sn-37Pb solder/copper interface were investigated using a solder-jointed plate specimen with a single-edge crack under mode I loading. The main conclusions obtained are summarized as follows:

1. Crack propagation rate (da/dN) could be characterized successfully by either stress intensity factor range (ΔK) or J-integral range (ΔJ). The threshold levels (ΔK_{th} and ΔJ_{th}), which represent the resistance of a material to fatigue crack growth, were 0.6 MPa.m$^{1/2}$ and 14 N/m, respectively.

2. Fatigue crack propagated in the solder parallel to the solder-copper interface and perpendicularly to the load direction. The manner of propagation is dominated by the cyclic-dependent FCG mechanism, i.e. transgranular manner of propagation through Pb-rich phases and Sn-rich phases.

3. With increasing crack length, the size of plastic zone reaches the interface and the stress exceeds the adhesive strength of interface, which results in the interfacial debonding. This debonding crack coalesces with the main crack and forms a crack along the interface, which unstably propagates in a brittle manner. The critical crack length (a/W) and adhesive strength for interfacial debonding were 0.46 and 20.2 MPa, respectively.

3.6 Acknowledgement

The authors would like to acknowledge discussions and supports from Dr. P. Dechaumphai, the Thailand Research Fund, the National Research Council of Thailand, and the National Metal and Materials Technology Center (Thailand).

3.7 References

Anderson, T.L., 1994. Fracture Mechanics: Fundamental and Applications, second ed. CRC Press, New York.

ASTM: E647, 1998. Standard Test Method for Measurement of Fatigue Crack Growth Rates. ASTM standards, The American Society for Testings and Materials. 03.01, 562-598.

Chiou, B.S., Chang, J.H., Duh, J.G., 1995. Metallurgical Reactions at the Interface of Sn/Pb Solder and Electroless Copper-Plated AlN Substrate. IEEE Transaction of Component, Hybrids and Manufacturing Technology-Part B. 18(3), 537-542.

Dundurs, J., 1969. Mathematical Theory of Dislocations. ASME, New York.

Hutchinson, J.W., Mear, M.E., Rice, J.R., 1987. Crack Paralleling an Interface between Dissimilar Materials. Journal of Applied Mechanics. 54, 828-832.

Hutchinson, J.W., Sou, Z., 1991. Mixed Mode Cracking in Layered Materials. Advance of Applied Mechanics. 29, 63-191.

Kanchanomai, C., Miyashita, Y., Mutoh, Y., 2002a. Low Cycle Fatigue and Mechanisms of a Eutectic Sn-Pb Solder 63Sn/37Pb. International Journal of Fatigue. 24, 671-683.

Kanchanomai, C., Miyashita, Y., Mutoh, Y., 2002b. Strain-rate Effects on Low Cycle Fatigue Mechanisms of a Eutectic Sn-Pb Solder. International Journal of Fatigue. 24(9), 987-993.

Kang, S.K., Sarkhel, A.K., 1994. Lead (Pb)-Free Solders for Electronic Packaging. Journal of Electronic Materials. 23(8), 701-708.

Lee, H., Chen, M., 2002. Influence of Intermetallic Compounds on the Adhesive Strength of Solder Joints. Materials Science and Engineering A. 333, 24-34.

Liu, J.H., Rice, D.W., Avery, P.A., 1987. Elastoplastic Analysis of Surface-Mount Solder Joints. IEEE Transaction of Component, Hybrids and Manufacturing Technology. 10(3), 346-357.

Logsdon, W.A., Liaw, P.K., Burke, M.A., 1990. Fracture Behavior of 63Sn-37Pb Solder. Engineering Fracture Mechanics. 36(2), 183-218.

Morris Jr., J.W., Freer Goldstein, J.L., Mei, Z., 1994. Microstructural Influences on the Mechanical Properties of Solder. in: Frear, D.R. (Eds.), The Mechanics of Solder Alloy Interconnects. Van Nostrand Reinhold, New York, pp. 7-41.

Nayeb-Hashemi, H., Yang, P., 2001. Mixed Mode I/II Fracture and Fatigue Crack Growth along 63Sn-37Pb Solder/Brass Interface. International Journal of Fatigue. 23, 325-335.

Pang, H.L.J., Tan, K.H., Shi, X.Q., Wang, Z.P., 2001. Microstructure and Intermetallic Growth Effects on Shear and Fatigue Strength of Solder Joints Subjected to Thermal Cycling Aging. Materials Science and Engineering A. 307(1-2), 42-50.

Quan, L., Frear, D., Grivas, D., Morris Jr., J.W., 1987. Tensile Behavior of Pb-Sn Solder/Cu Joints. Journal of Electronic Materials. 16(3), 203-208.

Rice, J.R., 1968. A Path Independent Integral and the Approximate Analysis of Strain Concentration by Notches and Cracks. Journal of Applied Mechanics. 35, 379-386.

Shih, C.F., Asaro, R.J., 1988. Elastic-Plastic Analysis of Cracks on Bimaterial Interfaces: Part I-Small Scale Yielding. Journal of Applied Mechanics. 55, 299-316.

Sou, Z., Hutchinson, J.W., 1989. Sandwich Test Specimens for Measuring Interface Crack Toughness. Materials Science and Engineering A. 107, 135-143.

Zhao, J., Mutoh, Y., Miyashita, Y., Ogawa, T., McEvily, A.J., 2001. Fatigue Crack Growth Behavior in 63Sn-37Pb and 95Pb-5Sn Solder Materials. Journal of Electronic Materials. 30(4), 415-421.

4. ผลที่ได้จากโครงการ

4.1 Mixed-mode fatigue crack growth specimens, which can represent the actual crack in solder joint.

4.2 Microstructural characteristics, composition, phase distribution, intermetallic analysis of Cu/63Sn-37Pb interface.

4.3 Stress intensity factor and *J*-integral ahead of crack tip.

4.4 Fundamental crack growth data, e.g. crack propagation rate, crack path, microstructure-crack relationship.

4.5 Fracture mechanics parameter to characterize fatigue crack propagation rate of solder under mixed-mode loading condition.

4.6 Adhesive strength of solder/copper interface.

4.7 Establish research group and facilities on fatigue and fracture mechanics in the Faculty of Engineering, Thammasat University.

4.8 Establish research corroboration between Thammasat University and Nagaoka University of Technology, Japan.

4.9 Results have been presented and published in the followings;

<u>C. Kanchanomai</u>, W. Limtrakarn, and Y. Mutoh, "Fatigue crack growth behavior in Sn-Pb eutectic solder/copper joint under mode I loading", Mechanics of Materials, in press (impact factor: 1.422).

<u>C. Kanchanomai</u>, "Fatigue Crack Growth along Sn-Pb Eutectic Solder/Copper Interface under Opening-Mode Loading", Mechanical Engineering Network of Thailand: The 17th Conference, Prachinburi, October 15-17, 2003.

5. ภาคผนวก

C. Kanchanomai, W. Limtrakarn, and Y. Mutoh, "Fatigue crack growth behavior in Sn-Pb eutectic solder/copper joint under mode I loading", Mechanics of Materials, in press (impact factor: 1.422).

C. Kanchanomai, "Fatigue Crack Growth along Sn-Pb Eutectic Solder/Copper Interface under Opening-Mode Loading", Mechanical Engineering Network of Thailand: The 17th Conference, Prachinburi, October 15-17, 2003.

MECMAT 1354
12 May 2005 Disk Used

ARTICLE IN PRESS

No. of Pages 9, DTD=5.0.1

Available online at www.sciencedirect.com
SCIENCE @ DIRECT

Mechanics of Materials xxx (2005) xxx–xxx

MECHANICS OF MATERIALS

www.elsevier.com/locate/mechmat

Fatigue crack growth behavior in Sn–Pb eutectic solder/copper joint under mode I loading

C. Kanchanomai [a,*], W. Limtrakarn [a], Y. Mutoh [b]

[a] Department of Mechanical Engineering, Faculty of Engineering, Thammasat University, Pathumthani 12120, Thailand
[b] Department of Mechanical Engineering, Nagaoka University of Technology, 1603-1 Kamitomioka, Nagaoka 940-2188, Japan

Received 31 March 2004

Abstract

Fatigue crack growth (FCG) behavior along 63Sn–37Pb solder/copper interface was investigated using a solder-jointed plate specimen with a single-edge crack under opening tensile loading (mode I). Finite element analysis was conducted for evaluating stress intensity factor (K) and J-integral (J) of the crack tip. Under frequency of 10 Hz and stress ratio of 0.1, the fatigue crack propagation rate could be characterized successfully by either stress intensity factor range (ΔK) or J-integral range (ΔJ). A fatigue crack propagated in transgranular manner through Pb-rich phases and Sn-rich phases near the solder/copper interface. With increasing crack length, the size of plastic zone at the crack tip and the von Mises stress along the solder/copper interface increased, which resulted in the interfacial debonding near the crack tip. The critical crack length (a/W) and adhesive strength for interfacial debonding were 0.46 and 20.2 MPa, respectively.

Keywords: Fatigue crack growth; Sn–Pb eutectic solder; Solder joint; Solder/copper interface; Adhesive strength

1. Introduction

Eutectic Sn–Pb solders have been widely used for electrical joints because of their low melting points, good wettability, good plasticity, reasonable electrical conductivity (Kang and Sarkhel, 1994). Due to their low melting temperature, the room temperature corresponds to a high homologous temperature (greater than 0.5). It is known that the time-dependent mechanisms, e.g. grain boundary sliding, cavitation and phase transformation, are possible to occur during fatigue test under high homologous temperature condition. These damage processes lead to premature failure when compared to cyclic-dependent fatigue failure, and life under low cycle fatigue (LCF) is dominated

* Corresponding author. Tel.: +66 02 564 3001; fax: +66 02 564 3010.
E-mail address: kchao@engr.tu.ac.th (C. Kanchanomai).

0167-6636/$ - see front matter © 2005 Elsevier Ltd. All rights reserved.
doi:10.1016/j.mechmat.2005.02.002

by crack propagation (Kanchanomai et al., 2002a,b). Zhao et al. (2001) reported that the mode I fatigue crack growth (FCG) behavior of bulk Sn–Pb eutectic solder was dominantly cyclic dependence at low stress ratios and high frequencies, while time-dependent behavior became dominant at high stress ratios and low frequencies. For the single Sn–Pb eutectic solder ball lap joint specimens, it was observed that the fatigue life reduced with increasing the cycles of thermal cycling aging (−40 to 125 °C) and the fatigue crack propagated in the Pb-rich region adjacent to the intermetallic layer in the solder material (Pang et al., 2001). Based on the finite element analysis, the stress state of a solder joint in surface mount assemblies was a combination between normal and shear stress states (Liu et al., 1987), which results in the mixed-mode loading condition at the interfacial crack tip even when external loading is pure mode I or pure mode II (Nayeb-Hashemi and Yang, 2001). The proportion of normal and shear stresses at the interfacial crack tip depends on both distances ahead of the crack tip and the elastic mismatches across the interface (Hutchinson et al., 1987; Sou and Hutchinson, 1989; Hutchinson and Sou, 1991).

While extensive work has been carried out on LCF and FCG of bulk Sn–Pb eutectic solder under mode I and mode II loading, very little is known about FCG behavior and mechanism of crack along solder/substrate interface. In the present study, the FCG behavior and mechanisms of crack along 63Sn–37Pb solder/copper interface under mode I loading were investigated and compared with those of bulk Sn–Pb eutectic solder.

2. Specimen and experimental procedures

FCG test under mode I loading was conducted on a solder-jointed plate specimen with a single-edge notch, as shown in Fig. 1. To make a specimen, two copper bars (99.9 wt.%) were jointed together by Sn–Pb eutectic solder (63Sn–37Pb). Before soldering, the copper bars were cleaned in order to remove the oxides according to the following procedure. First, the surfaces of copper bars were lightly polished using 600-grit emery paper,

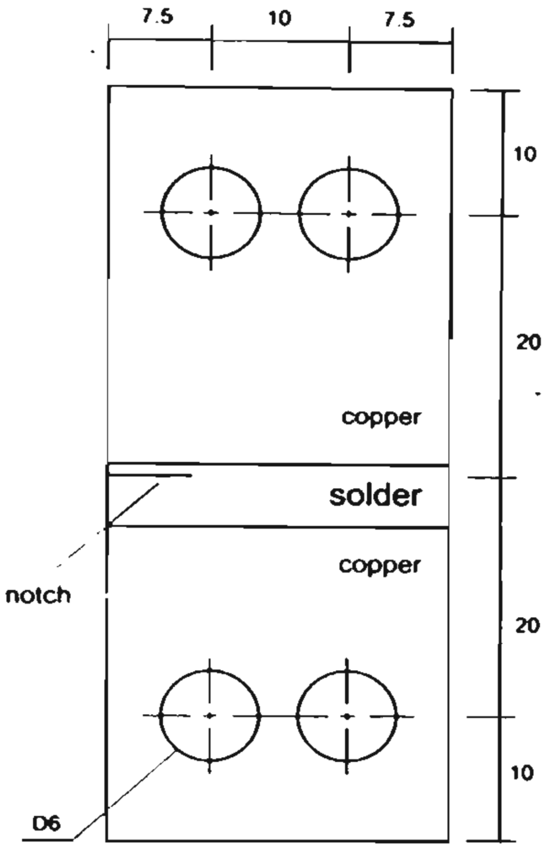

Fig. 1. Specimen geometry (6-mm thickness).

then dipped in a dilute nitric acid solution and rinsed in distilled water. The copper bars were coated with flux (Hakko 89-400, Japan) and placed in a special fixture made from nonsolderable material (aluminum alloy), as shown in Fig. 2. Bulk solder (63Sn–37Pb) was melted and reflowed into cavity between two copper bars. In order to allow the remaining flux to escape, the temperature of fixture and specimen was maintained at 250 °C (above solder reflow temperature) for 10 min before left to cool in air. By using this procedure, specimens can be manufactured with good alignment, a specific solder layer thickness, and a minimal void content. The excess solder was removed by milling and then lightly polished to obtain the geometry, as shown in Fig. 1. The geometry of specimen was designed in accordance with an ASTM recommendation

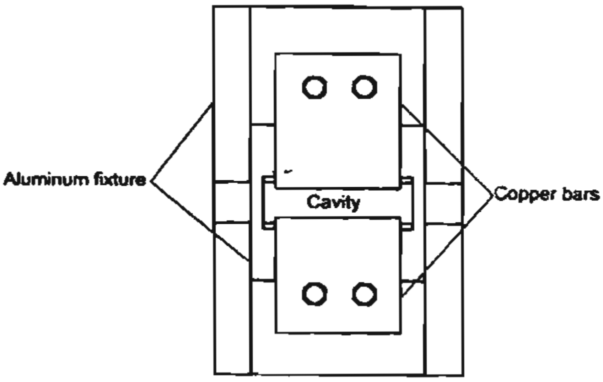

Fig. 2. Specimen reflow fixture.

(1998), i.e. $W/20 \leqslant B \leqslant W/4$, where W is the width and B is the thickness. The initial notch was introduced 1 mm far from the copper/solder interface by electro-discharge machining (EDM), and then the precracking (ASTM, 1998) was performed to obtain sharp initial crack ($a_0 = 0.25W$) before the FCG test.

FCG test was conducted in air at a constant temperature of 25 °C ($T/T_m > 0.5$), and a constant relative humidity of 55%. A servo-hydraulic fatigue machine (Instron 8872) with the load sensor capacity of 25 kN has been used in the present study. Cyclic loading was applied sinusoidally under a frequency of 10 Hz, a maximum load of 0.8 kN, and a load ratio of 0.1. Crack length was measured by using a traveling microscope with a precision of 10 μm. Scanning electron microscopy (SEM) and optical microscope examinations were performed directly on the specimens before and after tests.

3. Finite element analysis

According to the theory of fracture mechanics (Anderson, 1994), stress intensity factor (K) can be defined as the severity of the crack situation of a linear-elastic material as affected by crack size, stress, and geometry. For an interfacial crack under plane strain condition, the stress intensity factors in mode I and II (K_I and K_{II}) along the traction ahead of the crack tip ($\theta = 0$) are simply the real and imaginary parts of a complex stress intensity factor, whose physical meaning can be understood from the interface traction expressions (Hutchinson et al., 1987; Sou and Hutchinson, 1989):

$$(\sigma_{yy} + \mathrm{i}\sigma_{xy})_{\theta=0} = \frac{(K_I + \mathrm{i}K_{II})r^{\mathrm{i}\varepsilon}}{\sqrt{2\pi r}} \quad (1)$$

where, r and θ are polar coordinates centered at the crack tip. The x-axis coincides with the interface, while y-axis is perpendicular to the interface. The linear-elastic singularity solution in the crack tip region can be developed using the bimaterial constant (ε), defined as:

$$\varepsilon = \frac{1}{2\pi}\ln\frac{1-\beta}{1+\beta} \quad (2)$$

$$\beta = \frac{G_1(k_2 - 1) - G_2(k_1 - 1)}{G_1(k_2 + 1) + G_2(k_1 + 1)} \quad (3)$$

$$k = 3 - 4\nu \quad (4)$$

where, β is Dundurs' parameter (Dundurs, 1969), subscripts 1 and 2 refer to materials 1 and 2. G and ν are shear modulus of elasticity and Poisson's ratio, respectively.

Considering the low yield strengths of solders, i.e. below 20 MPa, a large plastic zone is possible to form ahead of the crack tip during FCG test. For such a condition, the energy release rate in a nonlinear elastic body that contains a crack, i.e. J-integral, can be used to describe crack tip conditions (Rice, 1968). The J-integral for an interfacial crack between two dissimilar isotropic materials under plane strain condition (Hutchinson and Sou, 1991), can be determined as follows

$$J = \frac{1-\beta^2}{E^*}(K_I^2 + K_{II}^2) \quad (5)$$

where

$$\frac{1}{E^*} = \frac{1}{2}\left(\frac{1}{\overline{E}_1} + \frac{1}{\overline{E}_2}\right) \quad (6)$$

$$\overline{E} = \frac{E}{(1-\nu^2)} \quad (7)$$

In the present work, finite element analysis (ABAQUS version 6.2-1) based on the interaction integral method (Shih and Asaro, 1988), was used to extract the individual stress intensity factors (K) and J-integral for a crack along solder/copper interface under plane strain condition. The mechanical properties of 63Sn–37Pb and copper used in the calculation are summarized in Table 1. The two-dimensional finite element model of the specimen (Fig. 3) consists of 2118 plane strain elements and 4,388 degrees of freedom (DOF). The maximum load of 0.8 kN and the stress ratio of 0.1 were used for the finite element analysis. The calculation results are shown in Fig. 4. The stress intensity factors (K) and J-integral increase with increasing crack length (a) in accordance with the basic theory of fracture mechanics (Anderson, 1994). The stress intensity factor range is in a combination between mode I and mode II, however the magnitude of K_I is significantly greater than that of K_{II}, i.e. K_I is the dominated fracture parameter for the present FCG test.

Table 1
Mechanical properties of solder and copper

Mechanical properties	63Sn–37Pb	Copper
Young's modulus (GPa)	32	134
Yielding strength (MPa)	18.1	140
Tensile strength (MPa)	39.7	295
Strain hardening exponent	0.30	-
Poisson's ratio	0.32	0.34

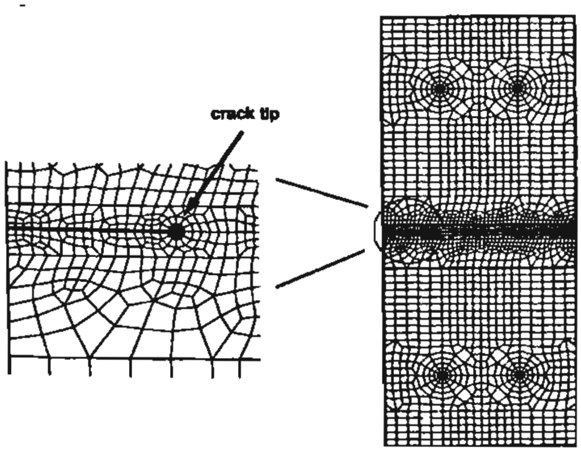

Fig. 3. Finite element mesh.

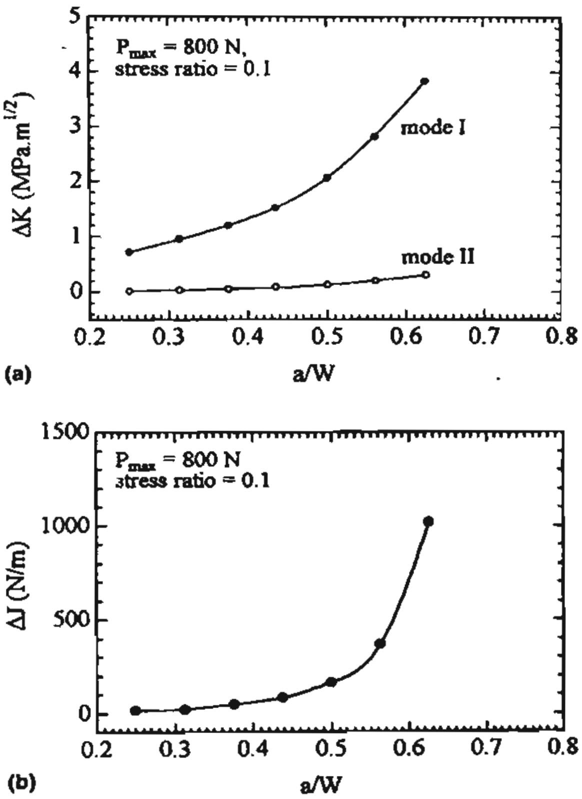

Fig. 4. Relationships between (a) stress intensity factor range and crack length, and (b) J-integral range and crack length.

4. Results and discussion

4.1. Microstructure

SEM micrograph of solder–copper interface is shown in Fig. 5. In the region of Sn–Pb eutectic solder, the microstructure consists of alternating phases of Pb (light) and β-Sn (dark), similar to those observed previously in the solder joints (Morris et al., 1994). Between solder and copper, the intermetallic layer due to the reaction between molten solder and copper surface could be observed. The intermetallic phase is a double layer of $Cu_3Sn(\varepsilon)$ on copper substrate and $Cu_6Sn_5(\eta)$ in contact with molten solder (Morris et al., 1994). Lee and Chen (2002) found that the activation energies of Cu_3Sn and Cu_6Sn_5 growth for 60Sn–40Pb are 59.2 kJ^{-1}mol and 42.25 kJ^{-1}mol,

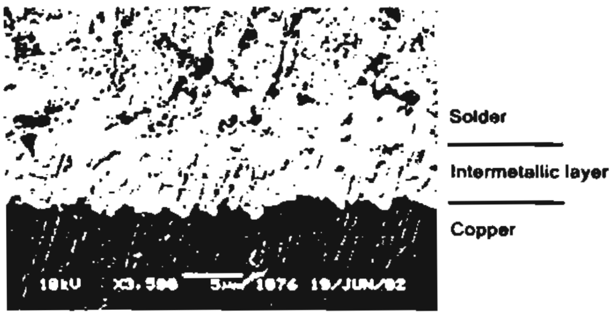

Fig. 5. Microstructures of the bonded interface.

respectively. Due to the lower activation energy, it is likely that the intermetallic layer was mainly the layer of Cu_6Sn_5 intermetallic. As seen from the Fig. 5, the intermetallic layer is about 8 μm in width and has a wavy profile along the interface. It should be noted that the variation of size and profile of intermetallic layer has some effects on adhesive and fatigue strength (Pang et al., 2001; Lee and Chen, 2002).

4.2. *Fatigue crack growth curve*

Relationship between crack length (a) and crack propagation rate (da/dN) is shown in Fig. 6a. The crack propagation rate increases with increasing crack length. The scattering of the data could be observed when the crack is short and it became less for the longer crack. In order to study the crack closure behavior, relationship between load and load-point displacement is plotted in Fig. 6b. No evidence of crack closure occurred during the FCG test, which is in accordance with the results reported previously by Logsdon et al. (1990).

Generally, if the plastic zone size at the crack tip (ω) is small relative to the local geometry, i.e. the small scale yielding condition ($\omega/a < 0.1$), the stress intensity factor (K) can be used without significant violation of the linear elastic fracture mechanics (LEFM) principals. For plane strain problem, the plastic zone size at $\theta = 0°$ crack plane can be estimated as follows

$$\omega = \frac{1}{3\pi}\left(\frac{K_I}{\sigma_y}\right)^2 \quad (8)$$

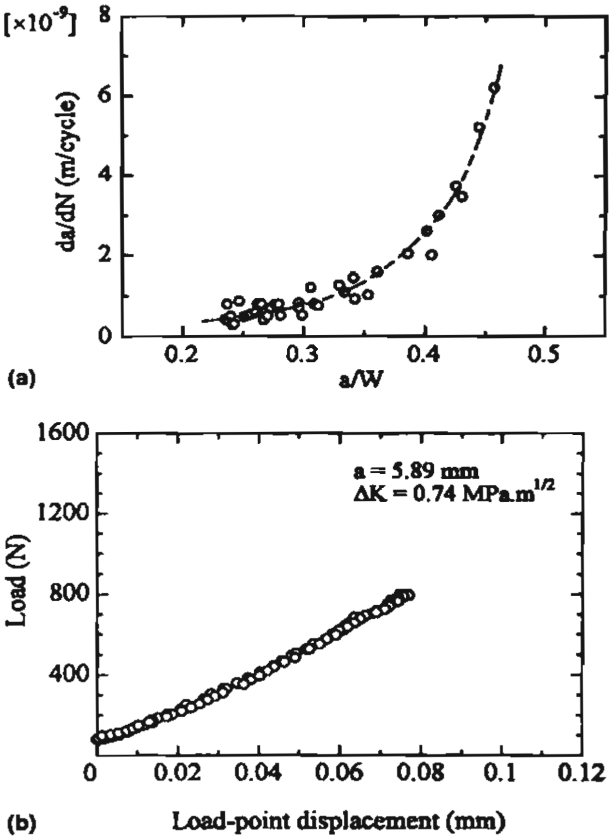

Fig. 6. (a) Relationship between crack length and crack propagation rate, and (b) relationship between load and load-point displacement.

where σ_y is the yield stress. From the estimation of the plastic zone size at $\theta = 0°$ crack plane, it was found that the ω/a ratio was less than 0.08 in the range of the present experiment. Therefore, the LEFM can be assumed to be valid and K can be used to characterize da/dN. For comparison purpose, the relationship between mode I stress intensity factor range (ΔK_I) and crack propagation rate (da/dN) is plotted in Fig. 7a together with that of bulk 63Sn–37Pb compact-tension specimen under the similar stress ratio and frequency (Zhao et al., 2001). From the figure, it can be seen that the present result correlates well with that of bulk 63Sn–37Pb solder.

However, the small scale yielding condition may not occur for the case of a small crack in actual solder joint. In such elastic–plastic situation,

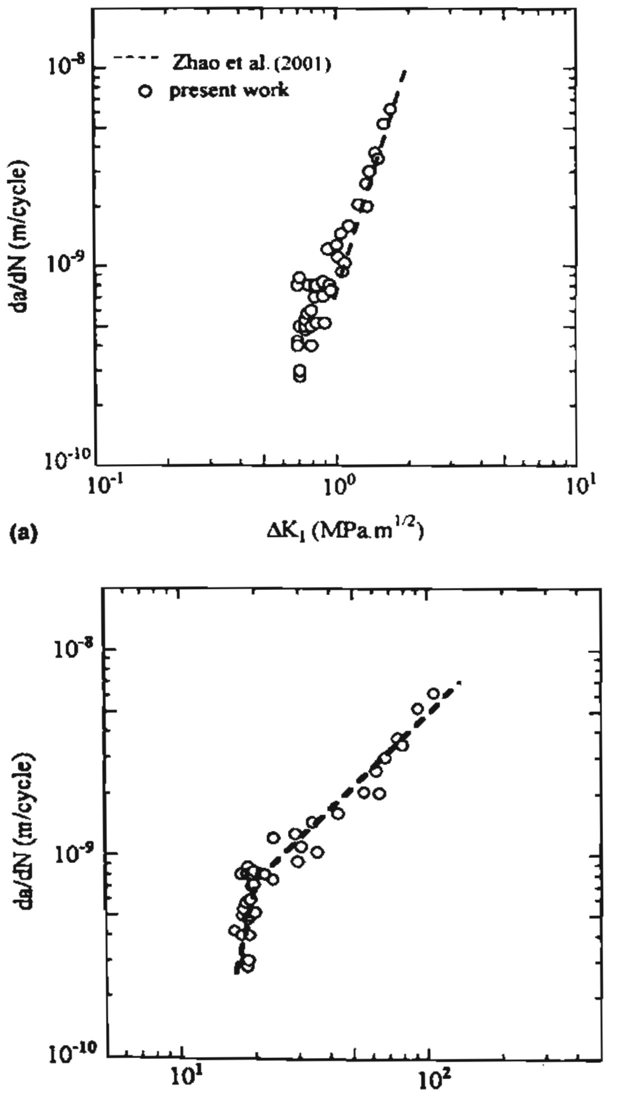

Fig. 7. Relationships between (a) stress intensity factor range and crack propagation rate, and (b) J-integral range and crack propagation rate.

ΔJ should be used as a fracture mechanics parameter instead of ΔK. The possibility of using ΔJ to characterize the FCG rate has been investigated and shown in Fig. 7b. It is seen that the data points lie on a double-slope line, which represents two regions: one where a crack grows at very slow rate, and the other where the relationship between ΔJ and da/dN is linear. As an importance characteristic to assess the resistance of a material to fatigue crack growth, the ΔJ and ΔK that correspond to the crack growth rate of 10^{-10} m/cycle are defined as ΔJ_{th} and ΔK_{th}, respectively (ASTM, 1998). By extrapolating the present fatigue crack growth curve to lower level, the estimated threshold value of J-integral range (ΔJ_{th}) is about 14 N/m, while that of stress intensity factor range (ΔK_{th}) is about 0.6 MPa m$^{1/2}$, which are in accordance with the results reported earlier by Zhao et al. (2001).

4.3. Fatigue crack path under interaction with interface

A crack initially propagated in the solder parallel to the solder–copper interface and perpendicularly to the load direction. As shown in Fig. 8, the crack propagated in transgranular manner, i.e. through Pb-rich phases (dark) and Sn-rich phases (light). Since the present FCG test was performed under low stress ratio and high frequency condition, it is likely that the manner of propagation is dominated by the cyclic-dependent FCG mechanism, i.e. transgranular manner of propagation (Zhao et al., 2001). Furthermore, the crack path is near the interface, only 1 mm far from it, which is much smaller than specimen width. The copper only elastically deforms in the present experiment, while the solder can plastically deform. Therefore, the region near the crack tip can-

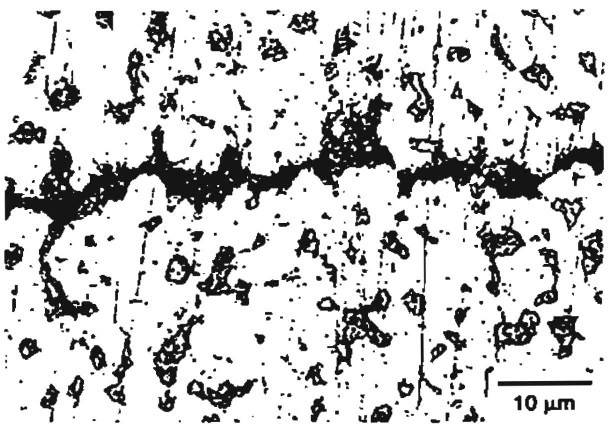

Fig. 8. Crack propagation path: Pb (dark) and β-Sn (light) (loading is in vertical direction).

not deform freely under the plastic constraint due to copper. It is reasonable that the plane strain condition can be assumed for the deformation near the interface of the present joint.

After some amount of crack propagation in the solder, the crack turned to the interface and propagated along the interface, as shown in Fig. 9. In order to investigate this growth phenomenon, the distribution of von Mises stress and strain near the crack tip at the maximum load for various crack lengths was estimated by using finite element analysis, as shown in Fig. 10. The discontinuity and irregular distribution of the stress and strain are mainly due to the difference of elastic modulus and yield strength between solder and copper. According to von Mises criterion, yielding occurs when von Mises stress reaches the uniaxial yield strength. Since the yield strength of the present solder is 18.1 MPa, the arrows in the solder region of

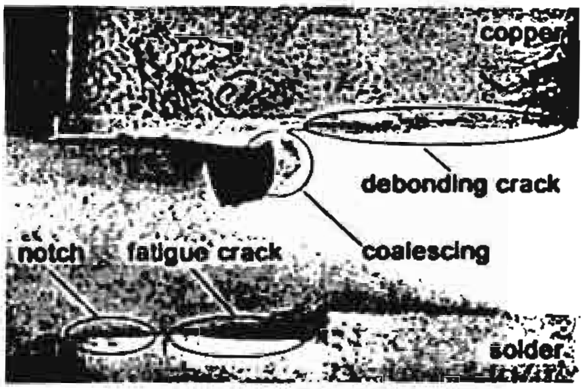

Fig. 9. Micrograph of final failure (loading is in vertical direction).

Fig. 10a–c indicate the plastic zone. The plastic deformation occurs only in the solder side, as can be seen from Fig. 10f. The distributions of von Mises stress and strain along the interface

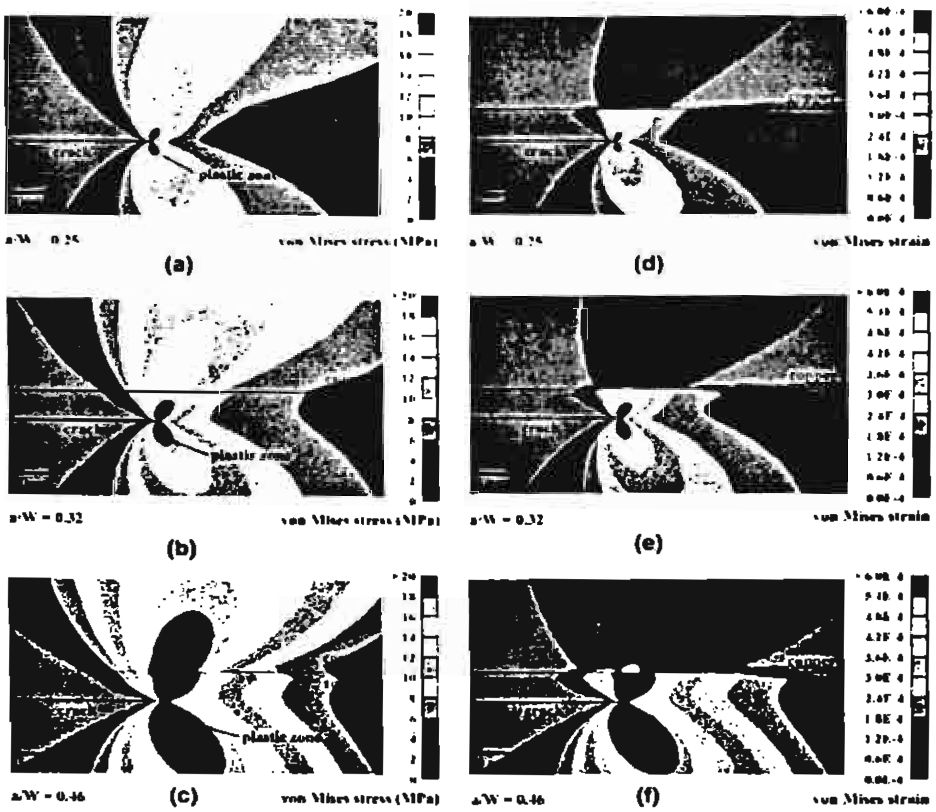

Fig. 10. von Mises stresses of the specimen for various crack lengths (a) $a/W = 0.25$, (b) $a/W = 0.32$, and (c) $a/W = 0.46$, and von Mises strains of the specimen for various crack lengths (d) $a/W = 0.25$, (e) $a/W = 0.32$, and (f) $a/W = 0.46$ (loading is in vertical direction).

are shown in Fig. 11a and b, respectively. It can be estimated from Fig. 11a that the plastic zone ahead of the crack tip reaches the interface when the crack length is longer than $a/W = 0.42$. Based on the experimental result, where the interface debonding occurs at the crack length of $a/W = 0.46$ (critical crack length), the interfacial von Mises stress, i.e. adhesive strength, can be estimated to be 20.2 MPa.

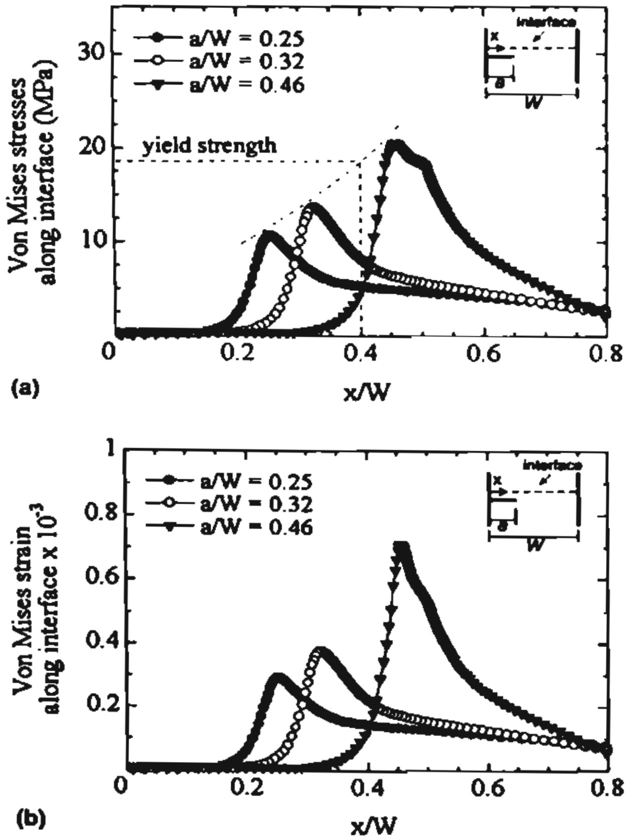

Fig. 11. (a) von Mises stresses along interface for various crack lengths, and (b) von Mises strains along interface for various crack lengths.

Quan et al. (1987) measured the adhesive strength of 60Sn–40Pb with a cross section of 3.18 × 7.62 mm by tensile test as 82.8 MPa, and became 46.23 MPa after storage at 250 °C for 6 h. Similar reduction in adhesive strength with increasing storage time was reported by Chiou et al. (1995), and Lee and Chen (2002). Since the size and profile of intermetallic band become thicker and rougher with the increasing storage time, it is likely that the adhesive strength depends on the size and profile of intermetallic band, i.e. become weaker with thicker and rougher intermetallic band, and results in the differences of the adhesive strength among literatures.

From the foregoing discussion, the crack growth behavior, where the crack turned to the interface and propagated along the interface after some amount of crack propagation in the solder, can be explained as follows. With increasing crack length, the size of plastic zone and the magnitude of stress near the crack tip increase. Consequently, the plastic zone reaches the interface and the stress exceeds the adhesive strength of interface, which results in the interfacial debonding, as schematically shown in Fig. 12. This debonding crack coalesces with the main crack and forms a crack along the interface, which unstably propagates in a brittle manner.

5. Conclusions

The behavior and mechanisms of FCG along 63Sn–37Pb solder/copper interface were investigated using a solder-jointed plate specimen with a single-edge crack under mode I loading. The main conclusions obtained are summarized as follows:

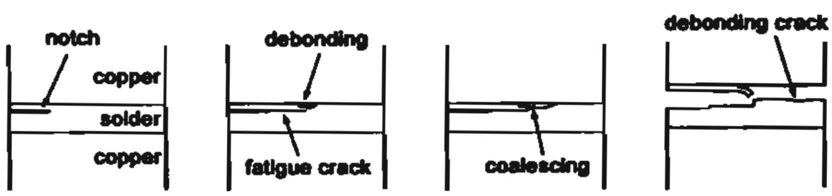

Fig. 12. Schematic of the crack propagation process.

1. Crack propagation rate (da/dN) could be characterized successfully by either stress intensity factor range (ΔK) or J-integral range (ΔJ). The threshold levels (ΔK_{th} and ΔJ_{th}), which represent the resistance of a material to fatigue crack growth, were 0.6 MPa m$^{1/2}$ and 14 N/m, respectively.
2. Fatigue crack propagated in the solder parallel to the solder–copper interface and perpendicularly to the load direction. The manner of propagation is dominated by the cyclic-dependent FCG mechanism, i.e. transgranular manner of propagation through Pb-rich phases and Sn-rich phases.
3. With increasing crack length, the size of plastic zone reaches the interface and the stress exceeds the adhesive strength of interface, which results in the interfacial debonding. This debonding crack coalesces with the main crack and forms a crack along the interface, which unstably propagates in a brittle manner. The critical crack length (a/W) and adhesive strength for interfacial debonding were 0.46 and 20.2 MPa, respectively.

Acknowledgments

The authors would like to acknowledge discussions and supports from Dr. P. Dechaumphai, the Thailand Research Fund, the National Research Council of Thailand, and the National Metal and Materials Technology Center (Thailand).

References

Anderson, T.L., 1994. Fracture Mechanics: Fundamental and Applications, second ed. CRC Press, New York.
ASTM: E647, 1998. Standard Test Method for Measurement of Fatigue Crack Growth Rates. ASTM standards, The American Society for Testings and Materials. 03.01, pp. 562–598.
Chiou, B.S., Chang, J.H., Duh, J.G., 1995. Metallurgical reactions at the interface of Sn/Pb solder and electroless copper-plated AlN substrate. IEEE Transaction of Component, Hybrids and Manufacturing Technology—Part B 18 (3), 537–542.
Dundurs, J., 1969. Mathematical Theory of Dislocations. ASME, New York.
Hutchinson, J.W., Mear, M.E., Rice, J.R., 1987. Crack paralleling an interface between dissimilar materials. Journal of Applied Mechanics 54, 828–832.
Hutchinson, J.W., Sou, Z., 1991. Mixed mode cracking in layered materials. Advance of Applied Mechanics 29, 63–191.
Kanchanomai, C., Miyashita, Y., Mutoh, Y., 2002a. Low cycle fatigue and mechanisms of a eutectic Sn–Pb solder 63Sn/37Pb. International Journal of Fatigue 24, 671–683.
Kanchanomai, C., Miyashita, Y., Mutoh, Y., 2002b. Strain-rate effects on low cycle fatigue mechanisms of a eutectic Sn–Pb solder. International Journal of Fatigue 24 (9), 987–993.
Kang, S.K., Sarkhel, A.K., 1994. Lead (PB)-free solders for electronic packaging. Journal of Electronic Materials 23 (8), 701–708.
Lee, H., Chen, M., 2002. Influence of intermetallic compounds on the adhesive strength of solder joints. Materials Science and Engineering A 333, 24–34.
Liu, J.H., Rice, D.W., Avery, P.A., 1987. Elastoplastic analysis of surface-mount solder joints. IEEE Transaction of Component, Hybrids and Manufacturing Technology 10 (3), 346–357.
Logsdon, W.A., Liaw, P.K., Burke, M.A., 1990. Fracture behavior of 63Sn–37Pb solder. Engineering Fracture Mechanics 36 (2), 183–218.
Morris Jr., J.W., Freer Goldstein, J.L., Mei, Z., 1994. Microstructural influences on the mechanical properties of solder. In: Frear, D.R. (Ed.), The Mechanics of Solder Alloy Interconnects. Van Nostrand Reinhold, New York, pp. 7–41.
Nayeb-Hashemi, H., Yang, P., 2001. Mixed mode I/II fracture and fatigue crack growth along 63Sn–37Pb solder/brass interface. International Journal of Fatigue 23, 325–335.
Pang, H.L.J., Tan, K.H., Shi, X.Q., Wang, Z.P., 2001. Microstructure and intermetallic growth effects on shear and fatigue strength of solder joints subjected to thermal cycling aging. Materials Science and Engineering A 307 (1–2), 42–50.
Quan, L., Frear, D., Grivas, D., Morris Jr., J.W., 1987. Tensile behavior of Pb–Sn solder/Cu joints. Journal of Electronic Materials 16 (3), 203–208.
Rice, J.R., 1968. A path independent integral and the approximate analysis of strain concentration by notches and cracks. Journal of Applied Mechanics 35, 379–386.
Shih, C.F., Asaro, R.J., 1988. Elastic–plastic analysis of cracks on bimaterial interfaces: Part I—Small scale yielding. Journal of Applied Mechanics 55, 299–316.
Sou, Z., Hutchinson, J.W., 1989. Sandwich test specimens for measuring interface crack toughness. Materials Science and Engineering A 107, 135–143.
Zhao, J., Mutoh, Y., Miyashita, Y., Ogawa, T., McEvily, A.J., 2001. Fatigue crack growth behavior in 63Sn–37Pb and 95Pb–5Sn solder materials. Journal of Electronic Materials 30 (4), 415–421.

การขยายตัวของรอยร้าวล้าบนรอยเชื่อมระหว่างโลหะบัดกรียูเทคติกดีบุก-ตะกั่วกับทองแดงภายใต้ภาระแบบเปิดผิวรอยร้าว

Fatigue crack growth along Sn-Pb eutectic solder/copper interface under opening-mode loading

ชาวสวน กาญจโนมัย
ภาควิชาวิศวกรรมเครื่องกล คณะวิศวกรรมศาสตร์ มหาวิทยาลัยธรรมศาสตร์
คลองหลวง ปทุมธานี 12121
โทร 0-25643001 ต่อ 3150 โทรสาร 0-25643010 E-mail: kchao@engr.tu.ac.th

Chaosuan Kanchanomai
Department of Mechanical Engineering, Faculty of Engineering, Thammasat University
Klong-Luang, Pathumthani 12121 Thailand
Tel: 0-25643001 Ext. 3150 Fax: 0-25643010 E-mail: kchao@engr.tu.ac.th

บทคัดย่อ

โลหะบัดกรียูเทคติกดีบุก-ตะกั่วได้ถูกใช้งานอย่างแพร่หลาย ในการเชื่อมต่อวงจรอิเล็กทรอนิกส์ของอุปกรณ์ไฟฟ้า ภายใต้สภาพอุณหภูมิสูงและอุณหภูมิที่เปลี่ยนแปลง การสะสมของความเสียหายตามจำนวนรอบของการเปลี่ยนแปลงอุณหภูมิซึ่งเรียกว่า"การล้า" เป็นสาเหตุหลักของความเสียหาย โดยอายุการล้ามีความสัมพันธ์กับอัตราการขยายตัวของรอยร้าว เมื่อทำการศึกษาการขยายตัวของรอยร้าวล้าบนรอยเชื่อมต่อระหว่างโลหะบัดกรียูเทคติกดีบุก-ตะกั่ว (63Sn-37Pb) โดยใช้ชิ้นทดสอบแบบ Compact tension shear (CTS) ภายใต้สภาพที่ผิวของรอยร้าวเปิดออกจากกัน (opening mode or mode I) และใช้ Finite element method คำนวณค่าพิสัยของตัวประกอบความเข้มของความเค้น (stress intensity factor range, ΔK) ของรอยร้าว ผลที่ได้แสดงให้เห็นว่า ค่าตัวประกอบความเข้มของความเค้นสามารถอธิบายอัตราการขยายตัวของรอยร้าวล้าบนรอยเชื่อมของโลหะบัดกรียูเทคติกดีบุก-ตะกั่วกับทองแดงภายใต้ภาระแบบเปิดผิวของรอยร้าวออกจากกันได้

Abstract

Eutectic Sn-Pb solder is extensively used for electrical and mechanical connection of electronic packagings. Under high homologous temperature and temperature cycling conditions, cumulative damage, i.e. fatigue, are likely to occur and life under fatigue is dominated by crack propagation. In the present study, fatigue crack growth (FCG) of 63Sn-37Pb solder/copper interface using a Compact Tension Shear (CTS) specimen under opening mode condition (mode I) was investigated. The finite element analysis based on the interaction integral method was used to extract the individual stress intensity factors for an interfacial crack. The results showed that the fatigue crack propagation rate of interfacial cracks could be characterized successfully by stress intensity factor ranges (ΔK).

1. Introduction

Eutectic Sn-Pb solders have been widely used for electrical joints because of their low melting points, good wettability, good plasticity, reasonable electrical conductivity [1]. Due to their low melting temperature, the room temperature corresponds to a high homologous temperature (greater than 0.5). Under high homologous condition, time-dependent mechanisms, e.g. grain boundary sliding, cavitation and phase transformation, are possible to occur. These damage processes lead to premature failure when compared to cyclic-dependent fatigue failure, and life under low cycle fatigue (LCF) is dominated by crack propagation [2, 3]. Zhao et al. [4] reported that the mode I fatigue crack growth (FCG) behavior of Sn-Pb eutectic solder was dominantly cyclic dependence at low stress ratios and high frequencies, while time-dependent behavior became dominant at high stress ratios and low frequencies. For the single Sn-Pb eutectic solder ball lap joint specimens, it was observed that the fatigue life reduced with increasing the cycles of thermal cycling aging (-40 to 125 °C) and the fatigue crack propagated in the Pb-rich region adjacent to the intermetallic layer in the solder material [5]. Under a four points bending test, it was found that the fracture toughness of the joint between 63Sn-37Pb/brass increased and fatigue crack growth rate (FCGR) decreased upon the introduction of the mode II component [6].

While extensive work has been carried out on fatigue behavior and FCG of bulk Sn-Pb eutectic solder, very little is known about FCG behavior solder/substrate interface. In the present study, FCG behavior and mechanisms of 63Sn-37Pb solder/copper interfaces under opening mode (mode I) are investigated experimentally.

2. Specimen and experimental procedures

Opening mode (mode I) fatigue crack growth studies were conducted on a Compact Tension Shear (CTS) specimen and loading device [7], as shown in Fig. 1. The forces acting on the holes of the CTS specimen are shown in Fig. 1b. Two copper bars (99.9 wt.%) were jointed together by Sn-Pb eutectic solder (63Sn-37Pb). Before soldering, the copper bars were cleaned in order to remove the residue solder and oxides according to the following procedure. First, the copper bars were heated above the solder reflow temperature using a high-wattage soldering iron, and the surfaces of copper bars were wiped. The surfaces of copper bars were lightly polished using 600-grit emery paper, then dipped in a dilute nitric acid solution and rinsed in distilled water. The copper bars were coated with flux (Hakko 89-400, made in Japan) and placed in a special fixture made from nonsolderable material (aluminum alloy), as shown in Fig. 2. Bulk solder (63Sn-37Pb) was heated and reflowed into cavity between two copper bars. In order to allow the remaining flux to escape, the temperature of fixture and specimen was maintained at 250 °C (above solder reflow temperature) for 10 minutes. The soldering iron was then removed, and the specimen was left to cool in air. The excess solder was removed by milling and then lightly polished to obtain the geometry, i.e. 25 mm-width (W) and 6 mm-thickness (B), as shown in Fig. 1b. The initial notch ($a_0 = 0.25W$) was introduced at the middle of specimen, i.e. 1 mm below copper-solder interface (Fig. 1a), by electro-discharge machining (EDM).

Fatigue crack growth (FCG) tests were conducted in air under a constant temperature of 25 °C ($T/T_m > 0.5$), and a constant relative humidity of 55%. A servo-hydraulic fatigue machine (Instron 8872) with the load sensor capacity of 25 kN has been used in the present study. During the tests, the maximum and minimum load magnitude acting on loading device were kept constant under a load ratio of 0.1, and cyclic loads were applied sinusoidally under a frequency of 10 Hz. Crack length was measured by using a traveling microscope with a precision of 10 μm. Scanning electron microscopy (SEM) and optical microscope examinations were performed directly on the specimens before and after tests

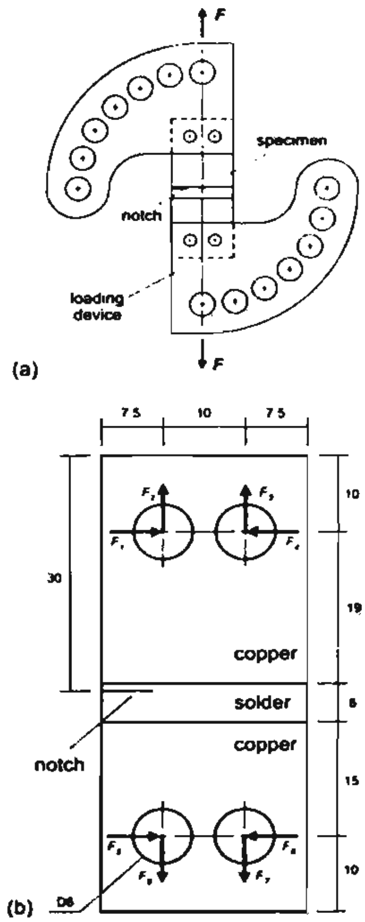

Fig. 1 (a) Loading device and (b) Specimen geometry (6 mm-thickness).

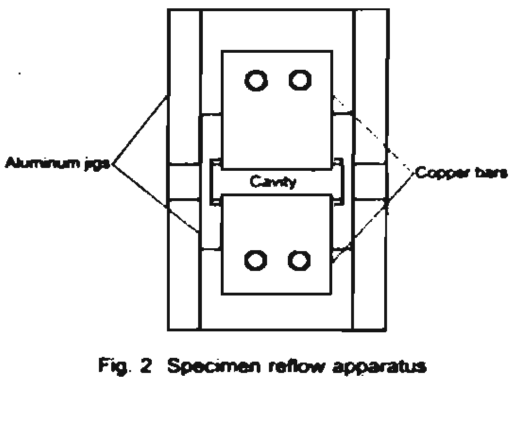

Fig. 2 Specimen reflow apparatus

3 Finite elements analysis

According to the theory of fracture mechanics [8], stress intensity factor (*K*) can be defined as the severity of the crack situation of a linear-elastic material as affected by crack size, stress, and geometry. For an interfacial crack, the stress intensity factors in mode I, II and III (K_I, K_{II} and K_{III}) along the traction ahead of the crack tip ($\theta = 0$) are simply the real and imaginary parts of a complex stress intensity factor, whose physical meaning can be understood from the interface traction expressions [9, 10]:

$$(\sigma_{22} + i\sigma_{12})_{\theta=0} = \frac{(K_I + iK_{II})r^{i\varepsilon}}{\sqrt{2\pi r}} \tag{1}$$

$$(\sigma_{23})_{\theta=0} = \frac{K_{III}}{\sqrt{2\pi r}} \tag{2}$$

where, r and θ are polar coordinates centered at the crack tip. The linear elasticity singularity solution in the crack tip region can be developed using the bimaterial constant (ε), defined as:

$$\varepsilon = \frac{1}{2\pi}\ln\frac{1-\beta}{1+\beta} \tag{3}$$

$$\beta = \frac{G_1(k_2-1)-G_2(k_1-1)}{G_1(k_2+1)+G_2(k_1+1)} \tag{4}$$

$$k = 3 - 4\nu \tag{5}$$

where β is Dundurs' parameter [11], subscripts 1 and 2 refer to material 1 and 2. ν and G are Poisson's ratio and shear modulus of elasticity, respectively.

In the present work, finite element analysis (ABAQUS version 6 2-1) based on the interaction integral method [12], was used to extract the individual stress intensity factors (*K*) for an interfacial crack. The mechanical properties of solder and copper used in the calculation are summarized in Table 1. The finite element model of the specimen (Fig. 3) consists of 2118 plane strain elements and 4,388 degrees of freedom (DOF). The maximum load of 0 8 kN and the boundary condition, which represents the loading condition as shown in Fig. 1a, are used for the finite element analysis. The calculation results are shown in Fig 4. The stress intensity factors (*K*) increases with increasing crack length (*a*) in accordance with the basic theory of fracture mechanics [8]

Table 1 Mechanical properties of solder and copper

Mechanical properties	63Sn-37Pb	Cu
Young's modulus (GPa)	32	115*
Yielding strength (MPa)	18 1	140*
Tensile strength (MPa)	39 7	345*
Poisson's ratio	0 324	0 37*

* reference [13]

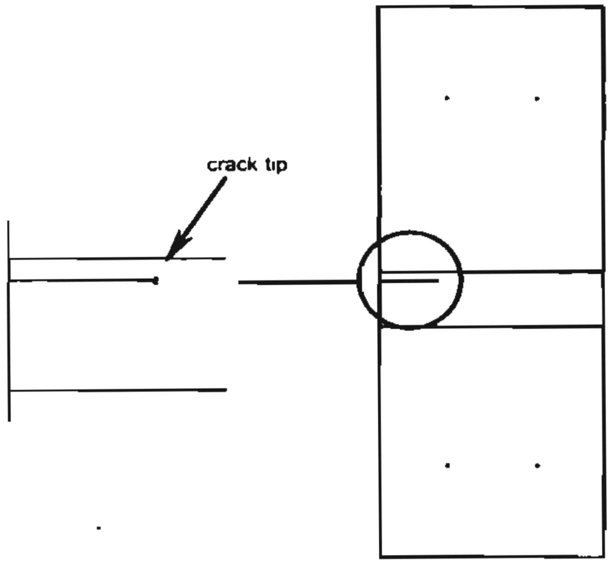

Fig. 3 Finite element mesh for specimen

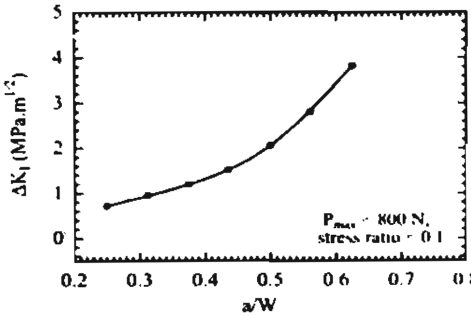

Fig. 4 Relationship between stress intensity factor range and crack length.

4. Experimental Results and Discussion

4.1 Microstructure

Microstructure of solder-copper interface, observed by an SEM, are shown in Fig. 5. In the region of Sn-Pb eutectic solder, the microstructure consists of alternating phases of Pb (light) and β-Sn (dark), similar to those observed previously in the solder joints [14]. Between solder and copper, the intermetallic layer dues to the reaction between molten solder and copper surface could be observed. The intermetallic phase is a double layer of Cu_3Sn (ε) on copper substrate and Cu_6Sn_5 (η) in contact with molten solder [14] Lee and Chen [15] found that the activation energies of Cu_3Sn and Cu_6Sn_5 growth for 60Sn-40Pb are 59 2 kJ/mol and 42 25 kJ/mol, respectively. Due to the lower activation energy, it is likely that the intermetallic layer was mainly the layer of Cu_6Sn_5 intermetallic

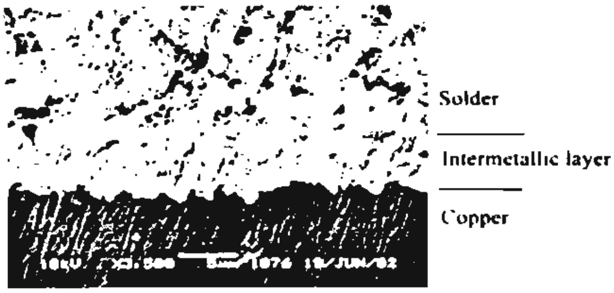

Fig. 5 Microstructures of specimen.

4.2 Fatigue crack path

The propagation path of the crack is shown in Fig. 6. Crack propagated from the notch closely to the solder-copper interface and perpendicularly to the load direction (mode I condition). Propagation of the crack was in transgranular manner, i.e. through Pb-rich phases (dark) and Sn-rich phases (light). Since the present FCG test was performed under low stress ratio and high frequency condition, it is resonable that the manner of propagation is affected by the cyclic-dependent FCG mechanism, i.e. transgranular manner of propagation [4].

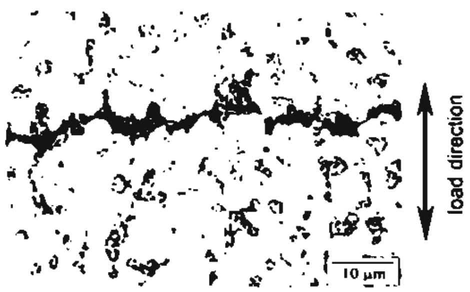

Fig 6 Crack propagation path, Pb (dark) and β-Sn (light).

4.3 Fatigue crack growth curves

Relationships between crack length (a) and crack propagation rate (da/dN) are shown in Fig. 7a. The crack propagation rate increases with the increasing crack length. The scattering of the data could be observed where the crack is short and became less for the longer crack. In order to study the crack closure behavior, the load and load-point displacement are plotted in Fig 7b. No evidence of crack closure could be observed during the FCG test, which is in accordance with the result reported previously by Logsdon et al [15].

For comparison, the relationship between stress intensity factor range (ΔK) and crack propagation rate (da/dN) of the present study is plotted in Fig 8 together with that of the bulk 63Sn-37Pb compact-tension specimen tested under similar stress ratio and frequency [4]. Although it is recognized that the large scale yielding condition existed during a portion of the present FCG test, the results correlates well with that of bulk 63Sn-37Pb solder. The threshold level could be obtained by extrapolating the plot in Fig 8 to a da/dN of 10^{-11} m/cycle [17]. The threshold value of stress intensity factor range (ΔK_{th}), which is an importance characteristic to assess the resistance of a Sn-Pb eutectic solder to fatigue crack growth, is 0.7 MPa m$^{1/2}$. This magnitude is in accordance with the magnitude reported earlier by Zhao et al. [4].

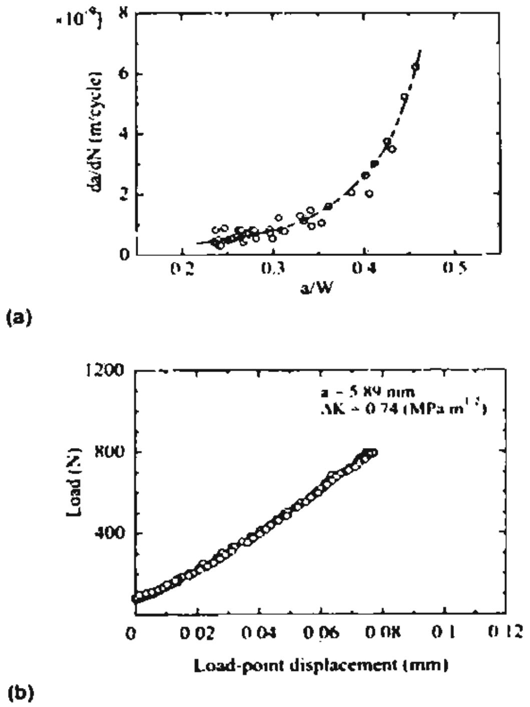

Fig. 7 (a) Relationship between crack length and crack propagation rate, and (b) Relationship between load and load-point displacement.

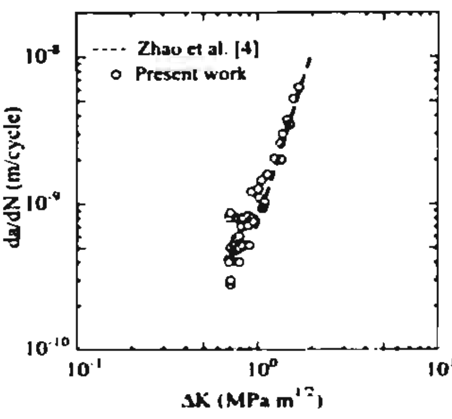

Fig 8 Relationship between stress intensity factor range and crack propagation rate

5. Conclusion

Fatigue crack growth behavior and mechanisms of 63Sn-37Pb solder/copper interfaces under opening mode (mode I) have been investigated at a constant temperature of 25 °C (T/T_m > 0.5). The intermetallic layer, dues to the reaction between molten solder and copper surface, was mainly the layer of Cu_6Sn_5 intermetallic. Fatigue crack propagated from the notch closely to the solder-copper interface and perpendicularly to the load direction (mode I condition). Propagation of the crack was in transgranular manner, i.e. through Pb-rich phases and Sn-rich phases. Crack propagation rate (*da/dN*) could be characterized successfully by stress intensity factor range (ΔK), calculated from the finite element method. The threshold levels (ΔK_{th}), which represent the resistance of a material to fatigue crack growth, were 0.7 MPa.m$^{1/2}$.

6. Acknowledgement

The author would like to acknowledge the financial support from the Thailand Research Fund, and thank Dr. Y. Mutoh for many fruitful discussions.

7. References

[1] S.K. Kang and Sarkhel A.K., "Lead (Pb) - Free Solders for Electronic Packaging", Journal of Electronic Materials, 1994, Vol. 23, No. 8, pp. 701-707.

[2] C. Kanchanomai, Miyashita Y., and Mutoh Y., "Low Cycle Fatigue and Mechanisms of a Eutectic Sn-Pb Solder 63Sn/37Pb", International Journal of Fatigue, 2002, Vol. 24, pp. 671-683.

[3] C. Kanchanomai, Miyashita Y., and Mutoh Y., "Strain-rate Effects on Low Cycle Fatigue Mechanisms of a Eutectic Sn-Pb Solder", International Journal of Fatigue, 2002, Vol. 24, No. 9, pp. 987-993.

[4] J. Zhao, Mutoh Y., Miyashita Y., Ogawa T., and McEvily A.J., "Fatigue Crack Growth Behavior in 63Sn-37Pb and 95Pb-5Sn Solder Materials", Journal of Electronic Materials, 2001, Vol. 30, No. 4, pp. 415-421.

[5] H.L.J. Pang, Tan K.H., Shi X.Q., and Wang Z.P., "Microstructure and Intermetallic Growth Effects on Shear and Fatigue Strength of Solder Joints Subjected to Thermal Cycling Aging", Materials Science and Engineering A, 2001, Vol. 307, No. 1-2, pp. 42-50.

[6] H. Nayeb-Hashemi and Yang P., "Mixed Mode I/II Fracture and Fatigue Crack Growth along 63Sn-37Pb Solder/Brass Interface", International Journal of Fatigue, 2001, Vol. 23, pp. 325-335.

[7] H.A. Richard and Benitz K., A Loading Device for the Creation of Mixed Mode in Fracture Mechanics. International Journal of Fracture, 1983. 22: p. R55-R58.

[8] T.L. Anderson, in Fracture Mechanics: Fundamental and Applications, 1994, CRC Press, New York, pp. 31-100.

[9] J.W. Hutchinson, Mear M.E., and Rice J.R., "Crack Paralleling an Interface between Dissimilar Materials", Journal of Applied Mechanics, 1987, Vol. 54, pp. 828-832.

[10] Z. Sou and Hutchinson J.W., "Sandwich Test Specimens for Measuring Interface Crack Toughness", Materials Science and Engineering A, 1989, Vol. 107, pp. 135-143.

[11] J. Dundurs, in Mathematical Theory of Dislocations, 1969, ASME, New York, pp. 70-115.

[12] C.F. Shih and Asaro R.J., "Elastic-Plastic Analysis of Cracks on Bimaterial Interfaces: Part I-Small Scale Yielding", Journal of Applied Mechanics, 1988, Vol. 55, pp. 299-316.

[13] ASM Handbook. Properties and Selection: Nonferrous Alloys and Special-Purpose Materials, ed. J.R. Davis. Vol. 2. 1990: ASM International.

[14] J.W. Morris Jr., Freer Goldstein J.L., Mei Z., "Microstructural Influences on the Mechanical Properties of Solder", in The Mechanics of Solder Alloy Interconnects, S.N.B. D.R. Frear, H.S. Morgan, and J.H. Lau, Editor. 1994, Van Nostrand Reinhold, New York. pp. 7-41.

[15] H. Lee and Chen M., "Influence of Intermetallic Compounds on the Adhesive Strength of Solder Joints", Materials Science and Engineering A, 2002, Vol. 333A, pp. 24-34.

[16] W.A. Logsdon, Liaw P.K. and Burke M.A., "Fracture Behavior of 63Sn-37Pb Solder", Engineering Fracture Mechanics, 1990, Vol. 36, No. 2, pp. 183-218.

[17] ASTM standards, ASTM E647-95a: Standard Test Method for Measurement of Fatigue Crack Growth Rates. The American Society for Testings and Materials, 1998, Vol. 03.01, pp. 562-598.